Wärme- und Stoffübertragung 12 (1979) 105-111

Wärme-und Stoffübertragung
Thermo- and Fluid Dynamics
© by Springer-Verlag 1979

Flow Model for Velocity Distribution in Fixed Porous Beds Under Isothermal Conditions

B.C. Chandrasekhara and D. Vortmeyer, München

Abstract. In a brief survey of the previous work the limitations of the modified Darcy equation and of the vectorial form of the Ergun equation are discussed. To include the effect of wall friction on the flows the viscous resistance term is added to the vectorial form of the Ergun equation. Using the generalized Ergun equation a one-dimensional formulation is presented for flow of fluids through packed beds taking into account the variation of porosity along the radial direction. It is found that there is a reasonable agreement between the numerical and the experimental results and it is observed that the variation of porosity with radial position has greater influence on channeling of velocity near the walls. For the assumption of constant porosity the velocity profiles exhibit similar nature as the plug flow profiles with a thin boundary layer near the wall.

Modell der Geschwindigkeitsverteilung in einem isotherm durchströmten Festbett

Zusammenfassung. In der vorliegenden Arbeit werden eingangs die Anwendbarkeitsgrenzen der modifizierten Darcy-Gleichung und der in vektorieller Form geschriebenen Ergun-Gleichung diskutiert. Um Einflüsse der Wandreibung auf eine Strömung mit in der Ergun-Gleichung berücksichtigen zu können, wird ein Reibungsterm hinzugefügt. Die so generalisierte Gleichung kann benutzt werden, um die eindimensional gerichtete Strömung durch eine Kugelschüttung zu berechnen. Eine radiale Veränderung der Schüttungsporosität ist dabei mit in die Betrachtung eingeschlossen. Das nichtlineare Grenzwertproblem wird numerisch gelöst und mit experimentellen Daten aus der Literatur verglichen. Die mit Meßwerten zufriedenstellend übereinstimmenden Rechenergebnisse zeigen, daß die radiale Porositätsverteilung in einem Festbett einen erheblichen Einfluß auf die Durchströmungsgeschwindigkeit in Wandnähe ausübt; die Berechnungen geben die Strömungsrandgängigkeit wieder. Wird die Bettporosität als unveränderlich angenommen, erhält man pfropfenströmungsähnliche Geschwindigkeitsprofile mit einer dünnen Wandgrenzschicht, in welcher die Geschwindigkeit auf den Wert null abfällt.

Nomenclature

A = Tridiagonal matrix defined in Eq. (20)
a = Bed radius
d_p = Particle diameter
f_1 = $150\,\mu(1-\varepsilon)^2/(\varepsilon^3 d_p^2)$ Darcy resistance term
f_2 = $1{,}75(1-\varepsilon)\rho/(\varepsilon^3 d_p)$ Parameter of resistance due to inertial effects
$\overline{f_1}$ = $150(1-\varepsilon)^2/\varepsilon^3$
$\overline{f_2}$ = $1{,}75(1-\varepsilon)/\varepsilon^3$
G = Column vector defined in Eq. (20)
k = Permeability, μ/f_1
L = Length of the bed
P = Pressure
r = Radial co-ordinate
R_p = Reynolds number based on particle diameter, $v_0 d_p/\nu$
$\vec{v}$, v_z = Superficial velocity vector, axial component
v_{1z} = Average superficial velocity defined in Eq. (20)
V = Absolute magnitude of velocity
$\bar{v}$ = The average velocity
v_0 = The velocity at the centre of the tube
X = Column vector defined in Eq. (20)
r^* = Dimensionless radial co-ordinate, r/a
p^* = Dimensionless pressure, $p/\rho v_0^2$
v_z^* = Dimensionless axial component of velocity, v_z/v_0
$\bar{v}^*$ = Dimensionless average velocity defined in Eq. (20)
z^* = Dimensionless axial co-ordinate, z/L

Greek letters

β = Ratio of tube radius to particle diameter, a/d_p
ε = Porosity or void fraction
ε_0 = Porosity at the axis of the container
μ = Dynamical viscosity
ν = Kinematic viscosity
ρ = Density
ξ = Distance from the wall of the container, defined in Eq. (16)

1 Previous Work

The study of flow through porous media is usually carried out using Darcy's law [1] given by the Equation

$$\nabla P = -\mu/k \vec{V} . \tag{1}$$

The above equation is valid in the regions away from the surface of the boundary and hence applied to large systems. In small systems the effect of wall friction is important and is responsible for skewing of the velocity profiles. It was Brinkman [2] who first incorporated the effect of boundaries into the equations of motion for flows through porous media by adding Darcy's resistance term to Stokes' equation. The equations of motion for Stokes-Darcy flow after Brinkman [2] are given by:

Continuity equation $\nabla \cdot \vec{V} = 0$. (2)

Momentum equation

$$-\nabla P + \mu \nabla^2 \vec{V} - \bar{\mu}/k \vec{V} = 0 \tag{3}$$

where $\bar{\mu}$ means an effective viscosity.

Later Tam [3] and Lundgren [4] derived Eq.(3) by rigorous mathematical approach using the ideas of statistical mechanics. In particular it was Lundgren who established that the effective viscosity is identical with the dynamical viscosity of the flow.

The modified Darcy equation derived by Lundgren [4] has the form

$$\mu \nabla^2 \vec{V} - \mu/k \vec{V} = \nabla P \tag{4}$$

where μ is the dynamical viscosity and k the permeability of the medium. The term $\mu\nabla^2\vec{V}$ is known as the viscous resistance term and the term μ/k is referred to as the Darcy resistance term. The viscous resistance term is effective in a scale length of $\delta = \sqrt{k}$ where the viscous resistance term and the Darcy resistance term have the same order of magnitude. In other words the boundary layer thickness in a porous medium is of order $\sqrt{k}$.

Equation (4) together with the continuity Eq.(2) describes the low velocity flow field in a porous medium. For the flow calculation in fixed beds with higher flow rates usually the linear Darcy law is replaced by the scalar non-linear Ergun [5] equation

$$-\partial P/\partial z = f_1 v_{1z} + f_2 v_{1z}^2 \tag{5}$$

where v_{1z} is the average superficial velocity and $\partial P/\partial z$ is the axial pressure gradient. Radestock and Jeschar [6] have performed flow calculation in fixed beds using the above scalar Eq.(5). Later Eq.(5) was written in vectorial form by Staneck and Szekely [7] as:

$$-\nabla P = \vec{V}(f_1 + f_2 V) \tag{6}$$

where $\vec{V}$ represents the point superficial velocity vector.

With the help of Eqs.(6) and (7) Szekely et al. [8, 9] have studied flow maldistribution which arises due to composite beds made of particles of various sizes, and non-uniform flows which result when the flows are introduced in a non-uniform manner.

However, Eq.(6) is not valid at the boundaries where the wall friction effect is important. To incorporate wall friction effects into the equations of motion we have introduced the viscous resistance term $\mu\nabla^2 V$ to the Ergun Eq.(6) as was done by Brinkman with Darcy equation. Hence the equations of motion which govern the fluid motion in fixed porous beds are

$$\mu\nabla^2\vec{V} - \nabla P = \vec{V}(f_1 + f_2 V) \tag{7}$$

$$\nabla \cdot \vec{V} = 0 \tag{8}$$

where $f_1 = \mu/k$. Equation (7) is the generalized vectorial form of Ergun equation which reduces to modified Darcy Eq.(4) when velocities involved are small, and describes low as well as high velocity flow fields in fixed beds.

2 Formulation of the Problem

The present work is confined to the study of one dimensional flow in isothermal fixed beds with a motive to explain the channeling of velocity profiles near the walls. The channeling of velocity profiles has important bearing on the better understanding of heat transfer problems as shown by Hennecke [10]. In the simple model of one dimensional flows considered only axial velocity v_z is important and is assumed to be a function of the radial co-ordinate r. One dimensional flows can be achieved in practise by making the bed sufficiently long and in which case all the radial velocities are assumed to vanish. The governing equations of motion for one dimensional flows, using Eqs. (7) and (8) are:

$$\mu\left(\frac{\partial^2 v_z}{\partial r^2} + \frac{1}{r}\frac{\partial v_z}{\partial r}\right) - \frac{\partial p}{\partial z} = f_1 v_z + f_2 v_z^2 \qquad (9)$$

$$\frac{\partial v_z}{\partial z} = 0 \, . \qquad (10)$$

Equation (10) is satisfied since the axial velocity is a function of r, only. The valid boundary conditions are:

The no-slip condition $v_z = 0$ at $r = a$ (11)

The symmetry condition $\frac{dv_z}{dr} = 0$ at $r = 0$. (12)

Introducing the non-dimensional quantities v*, p*, r*, z*, Eq.(9) is written as:

$$\frac{d^2 v_z^*}{dr^{*2}} + \frac{1}{r^*}\frac{dv_z^*}{dr^*} = \frac{dp^*}{dz^*} R_p \frac{a}{L} \beta + \overline{f_1} v_z^* \beta^2 + \overline{f_2} v_z^{*2} R_p \beta^2 . \qquad (13)$$

The transformed boundary conditions are:

$$v_z^* = 0 \quad \text{at} \quad r^* = 1 \qquad (14)$$

$$\frac{dv_z^*}{dr^*} = 0 \quad \text{at} \quad r^* = 0 \, . \qquad (15)$$

3 Solution for Beds of Uniform Porosity

First an analytical solution of Eq.(13) without the non-linear term, satisfying the boundary conditions (14) and (15) was obtained. Later a numerical solution of Eq.(13) in the presence of the non-linear term was also obtained.

The results of both these cases are presented in Fig.1. It is observed that in both cases the nondimensional axial velocity is flat except for a thin boundary layer near the wall, where the wall friction effects

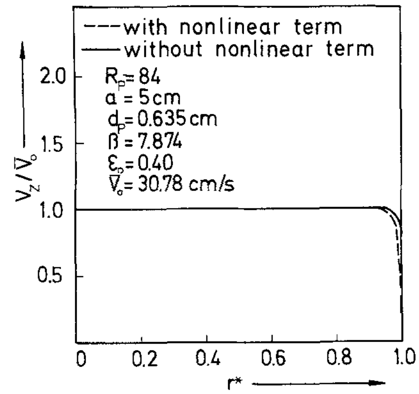

Fig.1. Velocity Vs Radial position for constant porosity

represented by the term $\mu\nabla^2\vec{V}$ become dominant. Further it is observed that the non-linear term in Eq.(13) increases the boundary layer thickness slightly. The overall nature of the velocity profile is that of a plug flow with a thin boundary layer. For reasons given below beds of uniform porosity have limited applications and do not represent a practical situation.

4 Radial Porosity Variation in a Fixed Bed

For constant porosity the axial velocity profiles are flat with a thin boundary layer near the walls. But the axial velocity measurements reported in literature [11, 12, 13] indicate that the axial velocity profiles exhibit channeling near the walls, that is, the velocity near the wall is maximum and approaches a constant value at the axis of the bed (Figs.2-6). Many workers who have measured the axial velocity have attributed the channeling of velocity near the walls to the variation of porosity along the radial distance. Hence in what follows a brief discussion on the variation of porosity is made.

Studies relating to void space distribution in randomly packed beds have been made by several authors. Notable among them are the measurements of Furnas [14], Thierney et al. [15], Schwartz and Smith [12] and Benenati and Brosilow [16]. Schwartz and Smith [12] have developed an equation which relates the porosity with velocity gradient, pressure gradient, void fraction at the centre of the bed and radial co-ordinates. The determination of porosity at any point in

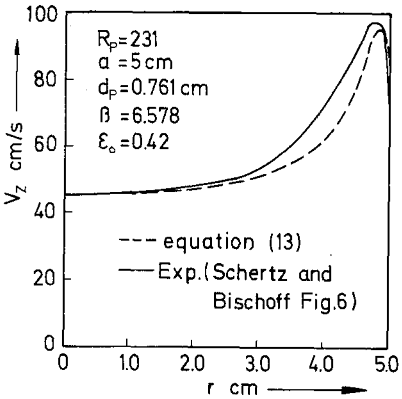

Fig.2. Velocity Vs Radial position

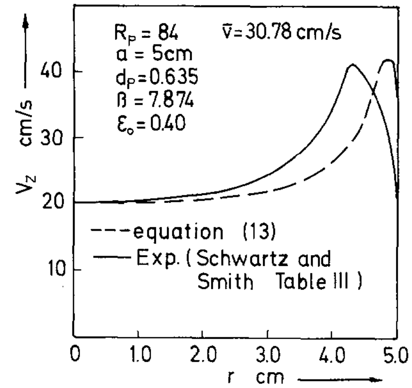

Fig.4. Velocity Vs Radial position

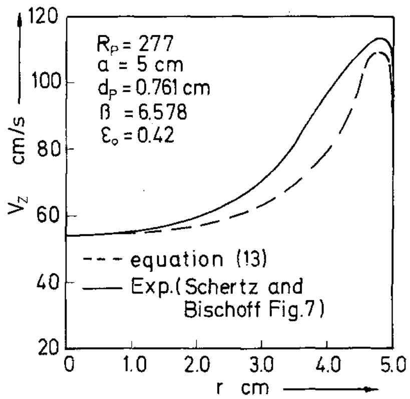

Fig.3. Velocity Vs Radial position

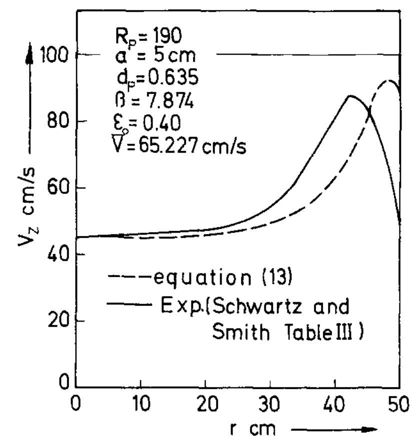

Fig.5. Velocity Vs Radial position

the bed involves a numerical stepwise integration. They have presented their numerical results corresponding to different particle sizes and different bed sizes in curves which are drawn to a void fraction of 0,32 at the center of the bed which they assume to be valid for all cases.

Further, they have calculated the void fraction only up to 2 sphere diameters from the wall of the container. Benenati and Brosilow [16] have established a graphical relationship between the spatial dependence of void fraction and radial position of the container in terms of particle diameter for different β. Use is made of Benenati's and Brosilow's results to establish an empirical relation between void fraction and the radial position r, which is useful for numerical computation. The results of integrated void fraction after Benenati and Brosilow exhibit an exponential variation with distance barring small oscillations. Hence the porosity can be represented by

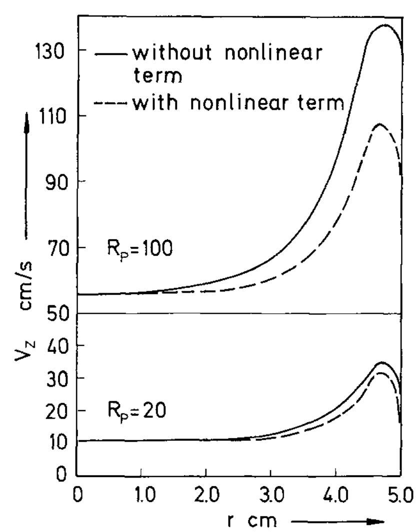

Fig.6. Velocity Vs Radial position

$$\varepsilon = \varepsilon_0(1 + b\,e^{-c\xi/dp}) \tag{16}$$

where ε_0 is the porosity at the centre of the bed, ξ is the distance from the wall and b and c are constant. Replacing ξ by the relation $\xi = a - r$, where a is the bed radius and r the radial co-ordinate, Eq. (16) is written in the form

$$\varepsilon = \varepsilon_0(1 + b\,e^{c(r/dp - a/dp)})$$

$$= \varepsilon_0(1 + b\,e^{c\beta(r^* - 1)}) \tag{17}$$

where $\beta = a/d_p$. By curve fitting the constants b and c are found to be b = 1 and c = 3 for $\beta = 7.0$ and $\beta = 10.5$. However suitable values of b and c are to be chosen for other values of β. Equation (17) is presented in Figs.7-8 along with the experimental results of Benenati and Brosilow and the theoretical results of Schwartz and Smith. It can be seen from Fig.7 that the theoretical results of Schwartz and Smith deviate much from the experimental results of Benenati and Brosilow as the centre of the container is approached.

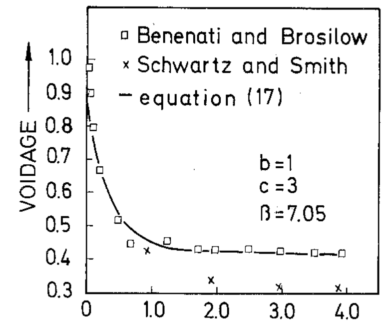

Fig.7. Voidage Vs Distance from the container wall (sphere diameters)

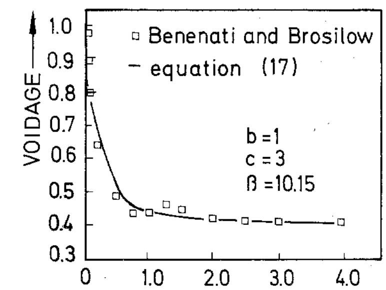

Fig.8. Voidage Vs Distance from the container wall (sphere diameters)

5 Assumption on Porosity Value Near the Wall

It is observed from Figs. 7 and 8 that the porosity or void fraction increases sharply between the wall and a distance of 1/4 sphere diameter from the wall. If the porosity relation as given by Eq.(17) is used for numerical solution it is found that the velocity profiles exhibit a sharp peak at the wall. The magnitude of the velocity is 3 to 4 times higher than the maximum experimental value and suddenly falls to zero at the wall. Also due to the sharp increase in porosity at the wall, the wall friction has no noticeable effect in reducing the velocity near the wall. On the contrary experimental profiles to exhibit a decrease in magnitude of velocity at the wall due to wall friction. Hence to obtain physically realistic velocity on the value of porosity at the wall is made. The maximum value of porosity is taken to be the value, given by Benenati and Brosilow's results, at a distance equal to slightly more than 1/4 sphere diameter from the wall and is assumed to have the same value up to the wall. Though this restriction on porosity appears to be a limitation of the present model yet the results based on this assumption agree with the experimentally observed axial velocity distribution indicating that the measurement of porosity near the wall needs careful consideration. The variation of porosity up to about 1/4 sphere diameter distance from the wall is given by

$$\varepsilon = \varepsilon_0(1 + b_1 e^{c_1\beta(r^* - r_1^*)}) \tag{18}$$

where r_1^* is the non-dimensional radial distance corresponding to 1/4 sphere diameter from the wall. In the present study the numerical solution of Eq.(13) is compared with the experimental works of Schertz and Bischoff and Schwartz and Smith. The non-dimensional distance corresponding to 1/4 sphere diameter distance from the wall is r = 0,96 for $\beta = 6{,}578$ (Schertz and Bischoff) and r = 0,9684 for $\beta = 7.874$ (Schwartz and Smith) with $\varepsilon_0 = 0{,}42$ and 0,4 respectively. To facilitate numerical computation Eq. (18) is written as

$$\varepsilon = \varepsilon_0(1 + b_1 e^{c_1\beta(r^* - 0{,}95)})\,. \tag{19}$$

The value of porosity at $r = 0,95$ is taken from Benenati and Brosilow results and they are equal to 0,588 and 0,56 for $\beta = 6,578$ and $\beta = 7,874$ respectively. The constants b_1 and c_1 in Eq.(19) have the values 0,4 and 0,931 respectively. It is to be noted that Szekely et al. [8] in their study have limited the porosity value adjacent to the wall to a maximum of 0,49 and do not mention at what distance from the wall the porosity has the above value.

6 Method of Solution

If porosity variation is included in Eq.(13) than it becomes a second order non-linear boundary value problem with variable coefficients. Since Eq.(13) cannot be solved analytically only numerical methods are to be tried. In the present study the method of quasilinearization Eq.(13) is transformed to the form

$$v_z^{*''}, n+1 + 1/r^* v_z^{*'}, n+1 - (\overline{f_1}\beta^2 + 2\overline{f_2}\,Rp\,\beta^2 v_z^*, n)\, v_z^*, n+1 = -\overline{f_2}\,Rp\,\beta^2 v_z^{*2}, n + d \qquad (20)$$

where v_z^*, n + 1 is the unknown value of v_z^* in a particular iteration step and v_z^*,n is the known value of v_z^* which should be prescribed initially when the iteration is started and $\partial p^*/\partial z^*\, \beta\, Rp\, a/L = d$. Equation (20) is then cast into finite difference form and written as

$$AX = G \qquad (21)$$

where A is a tridiagonal matrix, X and G are column vectors. To handle boundary conditions (14) and (15) grid points shifted from the boundaries are considered. To study the behaviour of the numerical solutions close to the wall 50 grid points are used and Eq.(21) is solved by Thomas algorithm. To start the iteration the value of v_z^*,n was taken to be zero in most of the cases. To see whether the initial non zero value of v_z^*,n has any effect on the final values of v_z^*,n+1, v_z^*,n was given initial values v_z^*,n=1, 2 and 3 and the iteration was performed. It was found that even when $v_z^*, n \neq 0$ the final values of iteration converged to the same values as in the case $v_z^*, n = 0$, establishing the stability of numerical results. The iteration was continued till there was sixth decimal place agreement between the final iterated values and the previous iterated values.

7 Comparison of Numerical Results with the Experimental Work of other Authors

The results of numerical solution of Eq.(13) are presented in Figs.2-6. For purposes of comparison with experimental results the results of Schertz and Bischoff and Schwartz and Smith obtained under isothermal conditions are used. Since the experiments were conducted at room temperature, the value of kinematic viscosity $\nu = 0,151$ at 293 °K is used to calculate the particle Reynolds number. To obtain numerical solution of Eq. (13) the value of the pressure gradient is required. For this purpose the pressure gradient required to produce the velocity v_0 at the centre of the container is calculated in each case from the scalar equation of Ergun without the $\mu\nabla^2\vec{V}$ term and is used for numerical calculation.

If v_0 is not known apriori then the following method can be adopted to calculate v_0. Generally $\bar{v}$, the average superficial velocity is known from the design data. v_0 is always less than $\bar{v}$. Assuming v_0 to be $0,6\,\bar{v}$ (say) to start with the pressure gradient required to produce $0,6\,v_0$ is calculated from the scalar Ergun equation. Using this pressure gradient the velocity profile is obtained from the numerical solution. To ensure that the velocity profile so obtained is correct the average velocity $\bar{v}$ is calculated from the mass balance equation

$$\bar{v}^* = \int_0^1 2 v_z^* r^* dr^* \qquad (22)$$

where $\bar{v}^* = \bar{v}/v_0$.

If the $\bar{v}$ calculated from Eq.(22) agrees with $\bar{v}$ which is known then the velocity profile obtained from the numerical solution is correct. If not, the value of v_0 is either increased or decreased and the process is repeated till $\bar{v}$, calculated from Eq.(22) agrees with $\bar{v}$ which is known to begin with. This process involves a number of trials to get at the correct v_0. However the computation time is about 1,5 seconds on CDC Cyber 175 for each trial and a number of trials can be made without involving excessive computation time to arrive at the correct v_0.

The results of numerical solution and experimental values of velocity measurements made by Schertz and Bischoff (Figs.2-3) agree reasonably well. However, the results of Schwartz and Smith (Figs.4-5) exhibit a peak in velocity away from the wall whereas the numerical solution indicates that the peak in velocity exists near the wall. Even physical considerations also point to the existence of the peak near the wall rather than away from the wall since the wall friction effects, which are the cause for the decrease of velocity, are dominant only near the wall. The results of Szekely et al. [8] and of Schertz and Bischoff support the above argument and the results of numerical solution of the present study.

The average velocity $\bar{v}$ using Eq.(22) was also calculated from the numerical solution and is compared with the results of Schwartz and Smith. Figure 4 represents the velocity profile for the average velocity $\bar{v}$ = 30,78 cm/sec. The numerical solution gives $\bar{v}$ = 26,7 cm/sec. Figure 5 represents the velocity profile for the average velocity $\bar{v}$ = 65.227 cm/sec. The numerical solution gives $\bar{v}$ = 59.76 cm/sec.

It is seen from Fig.6 that the effect of nonlinear term in Eq.(13) is to smooth the velocity profiles by reducing the peak near the wall. This effect is large for high particle Reynolds numbers and small for low particle Reynolds numbers. Comparing Fig. 1 and 2 we find that the variation of porosity has greater influence on channeling of velocity profiles near the walls than the inertial effects represented by the non-linear term in Eq.(13). Further, it is found that the ratio v_z/v_0 is independent of total flow rate which is in confirmity with the results of Schwartz and Smith.

8 Conclusions

With the $\mu\nabla^2\vec{V}$-term added to the vectorial form of the Ergun equation makes the Ergun equation to a generalized equation which reduces to the modified Darcy equation when the velocities involved are small and the medium is infinite in extent. Using the generalized Ergun equation the velocity distribution in an isothermal fixed bed can be predicted up to 1/4 sphere diameter from the wall incorporating the variation of porosity up to that distance.

Acknowledgement

The authors record their appreciation for the valuable discussion they had with Prof. Dr. N. Rudraiah, in the initial stages of the present work during his stay at the Technical University of Munich as a visiting professor.

Literature

1. Darcy, H.: Les fontaines publiques de la ville de Dijon. V. Dalmont, Paris (1856)
2. Brinkman, H.C.: Calculation of the viscous force exerted by a flow in fluid on a dense swarm of particles. Appl. Sci. Res. Section A1 (1947) 27
3. Tam, C.K.W.: The drag on a cloud of spherical particles in low Reynolds number flow. J.F.M. 38 (1969) 537
4. Lundgren, T.S.: Slow flow through stationary random beds and suspensions of spheres. J.F.M. 51 (1972) 273
5. Ergun, S.; Orning, A.: Fluid flow through randomly packed columns and fluidized beds. Ind. Eng. Che. 41 (1949) 1179
6. Radestock, J.; Jeschar, R.: Über die Strömung durch die Hochofenschüttung. Stahl Eisen 22 (1970) 1249
7. Staneck, V.; Szekely, J.: Three dimensional flow of fluids through nonuniform packed beds. AIChE J. 20, No. 5 (1974) 974
8. Szekely, J.; Poveromo, J.J.: Flow maldistribution in packed beds. A comparison of measurements with predictions. AIChE J. 21, No. 4 (1975) 769
9. Szekely, J. et al.: On the importance of the inertial terms in the modeling of flow maldistribution in packed beds. AIChE J. 22, No. 3 (1976) 600
10. Hennecke, F.W.: Über den Wandwiderstand beim Wärmetransport in Schüttungsrohren. Ph.D. Dissertation, University of Karlsruhe (1972)
11. Morales, M. et al.: Velocities and effective thermal conductivities in packed beds. Ind. Eng. Che. 45, No. 1 (1951) 225
12. Schwartz, C.E.; Smith, J.M.: Flow distribution in packed beds. Ind. Eng. Che. 45 No. 6 (1953) 1209
13. Schertz, W.M.; Bischoff, K.B.: Thermal and material transport in non-isothermal packed beds. AIChE J. 15 No. 4 (1969) 597
14. Furnas, C.C.: Flow of gases through beds of broken solids. Bull. 307 U.S. Bureau of mines (1929)
15. Roblee, L.H.S. et al.: Radial porosity variation in packed beds. AIChE J. 4, No. 4 (1958) 460
16. Benenati, R.F.; Brosilow, C.B.: Void fraction distribution in packed beds. AIChE J. 8, No. 3 (1962) 359
17. Carman, P.C.: Flow of fluids through porous materials. Butterworth, London (1956)

Dr. B.C. Chandrasekhara
Dept. of Physics
Centrale College
Bangalore University

Prof. Dr. rer. nat. D. Vortmeyer
Lehrstuhl B für Thermodynamik
Technische Universität München
Arcisstr. 21
D-8000 München 2

Received May, 23, 1978